2022

All-optical modulator based on a microfibre coil resonator functionalized with MXene

Pengfei Wang
Technological University Dublin, pengfei.wang@tudublin.ie

Shi Li
Harbin Engineering University

Fengzi Ling
Shenzhen University

See next page for additional authors

Recommended Citation
Pengfei Wang, Shi Li, Fengzi Ling, Gerald Farrell, Elfed Lewis, Yu Yin, All-optical modulator based on a microfibre coil resonator functionalized with MXene, Optical Fiber Technology, Volume 68, 2022, 102776, ISSN 1068-5200, DOI: 10.1016/j.yofte.2021.102776.

All-optical modulator based on a microfibre coil resonator functionalized with MXene

Pengfei Wang [a,b], Shi Li [b], Fengzi Ling [a], Gerald Farrell [c], Elfed Lewis [d], Yu Yin [b,*]

[a] Key Laboratory of Optoelectronic Devices and Systems of Ministry of Education and Guangdong Province, College of Optoelectronic Engineering, Shenzhen University, Shenzhen 518060, China
[b] Key Laboratory of In-fibre Integrated Optics of Ministry of Education, College of Physics and Optoelectronic Engineering, Harbin Engineering University, Harbin 150001, China
[c] Photonics Research Centre, Technological University Dublin, Dublin, Ireland
[d] Optical Fibre Sensors Research Centre, Department of Electronic and Computer Engineering, University of Limerick, Limerick, Ireland

ARTICLE INFO

Keywords:
Microfibre coil resonator
MXene
All-optical modulator

ABSTRACT

A novel all-optical modulator based on a microfibre coil resonator (MCR) functionalized using MXene is reported. The MCR was manufactured by winding a tapered fibre on a polycarbonate (PC) resin cylinder with low refractive index to support the microfibre, which also forms a fluidic channel coil. The MXene dispersion was injected into the channel to allow the deposition of an MXene layer using a photodeposition process. The transmission spectra were tuned using a tunable laser with a centre wavelength of 1550 nm and the light-matter interaction resulting from the photo-thermal effect and MXene absorption provide the all-optical modulation in this device. The variation of the resonance wavelength, phase shift and extinction ratio of transmission spectrum versus power were determined as 50 pm/mW, 0.262 π/mW and 0.554 dBm/mW respectively. The all-optical modulation properties were further characterized using a lens coupling method and adding a chopper to provide a controlled light source. The rise and fall response times for waveforms of the light signal were 0.179 and 0.145 ms, respectively. The intensity and width of the light signal waveform was modulated using the chopper-controlled light source, which indicates that MXene, as a new two-dimensional material, has excellent nonlinear optical effects and the MXene-MCR has the potential for use in ultra-fast optical nonlinear optical processing. The MXene-MCR has several superior characteristics compared with other all-optical modulators including excellent modulation properties, all-fibre construction, easy fabrication and fast response. These advantages demonstrate MXene-MCR has excellent potential for use as a tunable optical filter, an optical switch as well as an all-optical modulator.

1. Introduction

With the development of the fifth-generation mobile communication technology (5G), core communications networks demand higher data processing rates and transmission speeds. At present, the information processing at each node must undergo an optical-electrical-optical conversion as in traditional communication networks [1]. Faced with the demand for increasingly higher speeds and larger capacity, such conversions have a number of significant disadvantages that include bandwidth limitations, increased energy consumption and inflexibility in dense wavelength division multiplexed environments. Compared with traditional telecommunication networks, true end-to-end all-optical networks can effectively avoid these disadvantages and can offer large throughput capacity, a simpler network structure, improved reliability and the ability to be more easily reconfigured [2,3]. In the case of all-optical network information transmission, exchange and amplification do not require photoelectric and electro-optical conversion, which improves the communication speed and is no longer limited by the relatively slow response of electronic equipment, which effectively solves the existing “electronic bottleneck” problem in telecommunication networks [4,5].

A large amount of research has been undertaken to date to develop the devices needed to implement all-optical networks. In recent years, a large number of all-optical devices based on two-dimensional materials have been investigated including all-optical switches [6], all-optical threshold detectors [7], saturated absorbers (SA) [8] and optical

* Corresponding author.
E-mail address: cbyy@hrbeu.edu.cn (Y. Yin).

modulation [9]. Of particular value among all-optical devices are those that are based on optical fibres as such devices have the major advantage that interconnection to transmission fibres and other fibre devices is simple and reliable. Among such devices, all-fibre all-optical devices based on optical nonlinear effects have drawn extensive attention due to the wide range of possible applications in optical signal processing and optical communications [10–17]. Good examples include devices which can act as modulators, typically based on optical nonlinear effects. At present, the optical nonlinear effects used in all-fibre all-optical modulation include saturable absorption [18], the optical Kerr effect [19], stimulated Brillouin scattering [20], stimulated Raman scattering [21], the thermo-optic effect [22], free carrier accumulation[23]and free-carrier absorption[24–26]. However, due to the low nonlinear coefficient of conventional optical fibres, the modulation capability of optical fibre-based devices will be limited. Microfibres offer the potential for providing stronger nonlinear effects as an alternative to conventional optical fibres, given the increased interaction possible with their enhanced evanescent field, which in turn enhances the light-matter interaction and provides the possibility for efficient all-optical modulation [27]. As a type of microfibre device, microfibre resonators can be subdivided depending on their geometry: microloop (MLR), microknot (MKR) and microcoil based devices [28]. Among them, the microfibre coil resonator (MCR) has the superior features of a long coupling length, strong evanescent field, compact size and high stability. MCRs have been used as fibre sensors [29], fibre lasers [30], fibre couplers [31], all-optical tuning [32] and slow light systems [33].

In recent years, several two-dimensional (2D) materials have been proposed for use in all-optical modulators, including graphene [34], black phosphorus (BP) [35] and transition-metal dichalcogenides (TMDs) [36,37]. Graphene, as a freestanding 2D material, has many excellent optical properties, such as broadband absorption, ultra-high electron mobility etc. However, the inherently gapless band structure and low density of graphene has limited its application in the field of optoelectronics. TMDs (MoS_2, $MoSe_2$, WS_2, etc) exhibit a direct band gap, strong optical absorption and high electronic on/off ratios. However, low mobility and a band gap fixation limit their use in optical modulation. BP has excellent photonic and electronic properties, including high carrier mobilities, tunable band gaps, a wide spectral response, high electronic off/on ratios and high absorption efficiencies. However, the drawbacks of BP include a lack of stability and limited conductivity, which greatly limit its application in the field of opto-electronic devices. Recently, MXene has attracted much attention due to several advantages which include: high elastic modulus, high capacity, adjustable band gap and tunable optical properties. To date, MXene has been employed for use in all-optical modulators based on a Michelson interferometer (MI) [38], Mach-Zehnder interferometer (MZI) [39] and MKR [40]. However, these structures are easily affected by their environment which can cause structural changes, which in turn results in an undesirable drift of the modulation properties. Therefore, it is important to develop an all-optical modulator using a structure which has high stability and improved modulation properties.

In this article, an all-optical modulator based on an MCR functionalized with MXene (MXene-MCR) is demonstrated experimentally. The modulator was manufactured by winding a microfibre on a hollow rod of low refractive index polycarbonate (PC) resin and then injecting an MXene ($Ti_3C_2T_x$) dispersion in the presence of incident light using a photodeposition method. The MXene-MCR was irradiated using a tunable laser to assess the all-optical modulation response of the resonance wavelength and the extinction ratio as a result of the photothermal effect and optical absorption. The resonance wavelength, phase shift and extinction ratio modulation efficiency were measured as 50 pm/mW, 0.262 π/mW and 0.554 dBm/mW respectively. In order to further evaluate the modulation properties, the light path was altered by changing the fibre optic fusion splicing method to a lens coupling method and adding an optical chopper between the pump light source and the 90% port of an optical coupler. The frequency and duty cycle of waveforms for the light signal were the same as that of the pump light source, indicating that the light signal can be modulated using the pump light source. The rise and fall response time were 0.179 and 0.145 ms, respectively. The output intensity increases with increasing pump power and the waveform pulse width decreases with increasing the chopper frequency. The modulation efficiency might be further improved by adjusting the fabrication parameters of MCR and improving the MXene properties. The device has several advantages including excellent modulation performance, all-fibre construction, ease of fabrication, fast response and has the feasibility to be applied as a tunable optical filter, optical switch and all-optical modulator.

2. Experiment

Prior to functionalization of the MXene, 5 g of MXene $Ti_3C_2T_x$ nanosheet material (XFK08, 12363-89-2102654) was placed into 100 mL of deionized (DI) water and dispersed in the DI water following ultrasonic processing. The Transmission Electron Microscopy (TEM) image of the prepared MXene is shown in Fig. 1(a), which shows that the MXene exhibits a layered structure. Fig. 1(b) shows the UV–Vis-NIR transmission spectrum of the MXene dispersion when observed using a UV–Vis-NIR spectrophotometer (PerkinElmer, Lambda 900). It has a wide broadband transmission range from 600 nm to 2000 nm, which indicates that MXene has a wide absorption range, suggesting its potential for application in all-optical modulation.

The MXene-MCR fabrication process was divided into two stages, being initially MCR fabrication followed by MXene functionalization of the MCR. A standard single-mode optical fibre (Corning SMF-28) was used to draw a microfibre using a fused biconical taper method, which resulted in a waist diameter of 2.42 μm. A polymethyl methacrylate (PMMA) rod of 1 mm diameter and 2.5 cm length was coated with an Ultra Violet (UV)-curable low refractive index PC resin (Luvantix, PC373-LD) and cured using a UV lamp (Lightningcure, LC8). Then the rod was immersed in acetone for 12 h to dissolve the PMMA, resulting in a hollow PC resin cylinder to be used as a supporting rod for the MCR. The drawn microfibre was wrapped around the supporting rod to form an MCR with 4 turns and the gap between adjacent rings was measured to be 7.48 μm, as shown in Fig. 1(c). The coil structure was fixed in place using a coating of the same PC resin and fully cured. The prepared MCR was then placed on a glass slide coated with the same PC resin which was again fully cured so as to ensure mechanical stability and facilitate subsequent measurements. The fabricated all-optical modulation device consists of a 4-turn MCR structure surrounding a fluidic channel.

The experimental setup for functionalization and modulation effect assessment is shown in Fig. 2. The signal was provided using a superluminescent diode (SLD) source (Thorlabs, S5FC1005S). The excitation (pump) light was provided using a tunable laser (TL, Santec TSI-710). The signal and pump light were combined using a 90:10 optical coupler (OC, 1550 FBT Coupler), where the 90% port was connected to the TL and the 10% port to the SLD source. The output port was connected to the MCR. The MXene dispersion was injected into the fluidic channel using a syringe when subject to irradiation from the SLD source so that the MXene became attached to the inside of the fluidic channel based on photodeposition. The photodeposition is based on the strong evanescent field effect of the microfiber, which makes the cone region of the microfiber produce a strong light intensity gradient. At the same time, the evanescent field of the microfiber generates a gradient force on the tiny materials near the tapered area, so that the materials are deposited in the tapered area of the microfiber [41]. In the case of the MCR, the materials are deposited on the inside of the fluidic channel where the microfiber taper is located. The process of functionalization was conducted by injecting the MXene dispersion and allowing 6 h for curing as well as repeating 3 times to ensure that sufficient MXene is deposited in the fluidic channel.

Following deposition, the all-optical modulation properties of the MXene-MCR were characterised based on the output spectra, which

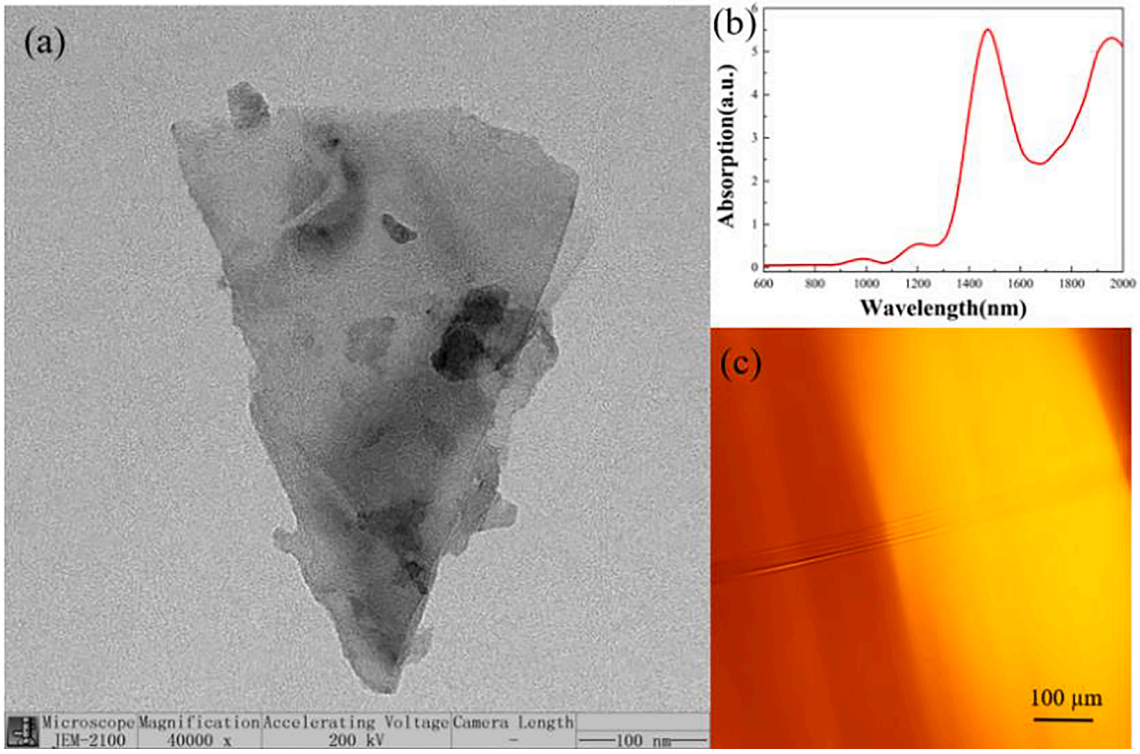

Fig 1. (a) TEM image of MXene nanosheets. (b) UV–Vis-NIR transmission spectrum of the $Ti_3C_2T_x$ MXene dispersion. (c) Microscope image of the MCR.

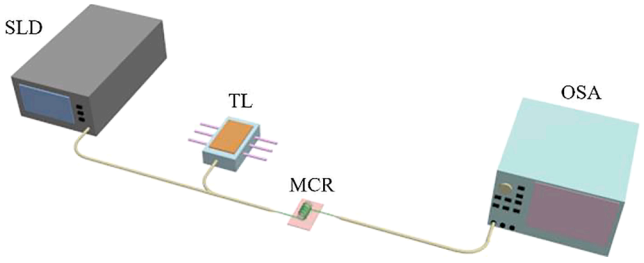

Fig 2. Experimental setup of MXene functionalization process and all-optical modulation based on MXene-MCR.

were measured using an optical spectrum analyzer (OSA, YOKOGAWA, AQ-6370C).

3. Results and discussion

Under illumination using the tunable laser, the transmission spectrum of MXene-MCR exhibits a variation with the change of pump light power, as shown in Fig. 3(a) over the range 0–5.65 mW. As the pump power increases from zero, the MCR resonance wavelength undergoes a red shift as a result of the photo-thermal effect and the extinction ratio increases due to optical absorption by the MXene. In order to assess the modulation capability, the correlation between the resonance wavelength shift, extinction ratio and pump power over the range 0–11.3 mW were measured and the results are shown in Fig. 3(b) and (c). It is evident that the resonance wavelength shift and extinction ratio increase linearly with increasing pump power. The sensitivities were measured as 50 pm/mW and 0.554 dBm/mW for the MXene-MCR. The phase shift is related to the resonance wavelength shift, with a phase shift sensitivity of 0.262 π/mW.

It is useful to explore the physical mechanism for all-optical tuning of the MXene-MCR and for this it was essential to consider optical transmission in the MCR. In MCR, there are two types of optical transmission paths: one is along the microfibre, and the other is coupled into the adjacent microfibre coils through the strong evanescent field, which can be expressed as follows [42]:

$$-\mathrm{i}\frac{d}{ds}\begin{bmatrix} A_1(s) \\ A_2(s) \\ A_3(s) \\ \vdots \\ A_{n-2}(s) \\ A_{n-1}(s) \\ A_n(s) \end{bmatrix} = \begin{bmatrix} 0 & c & 0 & 0 & \cdots & 0 & 0 & 0 & 0 \\ c & 0 & c & 0 & \cdots & 0 & 0 & 0 & 0 \\ 0 & c & 0 & c & \cdots & 0 & 0 & 0 & 0 \\ \vdots & \vdots & \vdots & \vdots & \vdots & \vdots & \vdots & \vdots & \vdots \\ 0 & 0 & 0 & 0 & \cdots & c & 0 & c & 0 \\ 0 & 0 & 0 & 0 & \cdots & 0 & c & 0 & c \\ 0 & 0 & 0 & 0 & \cdots & 0 & 0 & c & 0 \end{bmatrix} \begin{bmatrix} A_1(s) \\ A_2(s) \\ A_3(s) \\ \vdots \\ A_{n-2}(s) \\ A_{n-1}(s) \\ A_n(s) \end{bmatrix} \tag{1}$$

where $A_j(s)$ is the electric field amplitude of the j^{th} coil as a function of distance s around the coil and c is the coupling coefficient between two adjacent coils. The amplitude of the transmittance of the MCR can be defined as:

$$T = \frac{A_n(S)e^{i\beta S}}{A_1(0)} \tag{2}$$

where β is the propagation constant and S is the length of each coil. For the fundamental mode, the eigenvalue equation can be expressed as [43]:

$$\left[\frac{J_1^{'}(U)}{UJ_1(U)} + \frac{K_1^{'}(W)}{WK_1(W)}\right]\left[\frac{J_1^{'}(U)}{UJ_1(U)} + \frac{n_2^2 K_1^{'}(W)}{n_1^2 WK_1(W)}\right] = \left(\frac{\beta}{kn_1}\right)^2\left(\frac{V}{UW}\right)^4 \tag{3}$$

where n_1 is the refractive index (RI) of the fibre, n_2 is the RI of the surrounding environment, U is the normalized transverse phase parameter, V is the normalized frequency, W is the normalized lateral attenuation parameter and k is the wave vector.

As the pump light propagates in the MXene-MCR, the combined influence of the photo-thermal effect and absorption of the MXene result in all-optical modulation. The pump light results in a temperature increase of MXene due to the photo-thermal effect and the excess energy is diffused into the MCR [44] as heat transfer. The real part of the refractive index of MXene is affected by the temperature change via the thermo-optic effect of the material [45]. Therefore, the refractive index

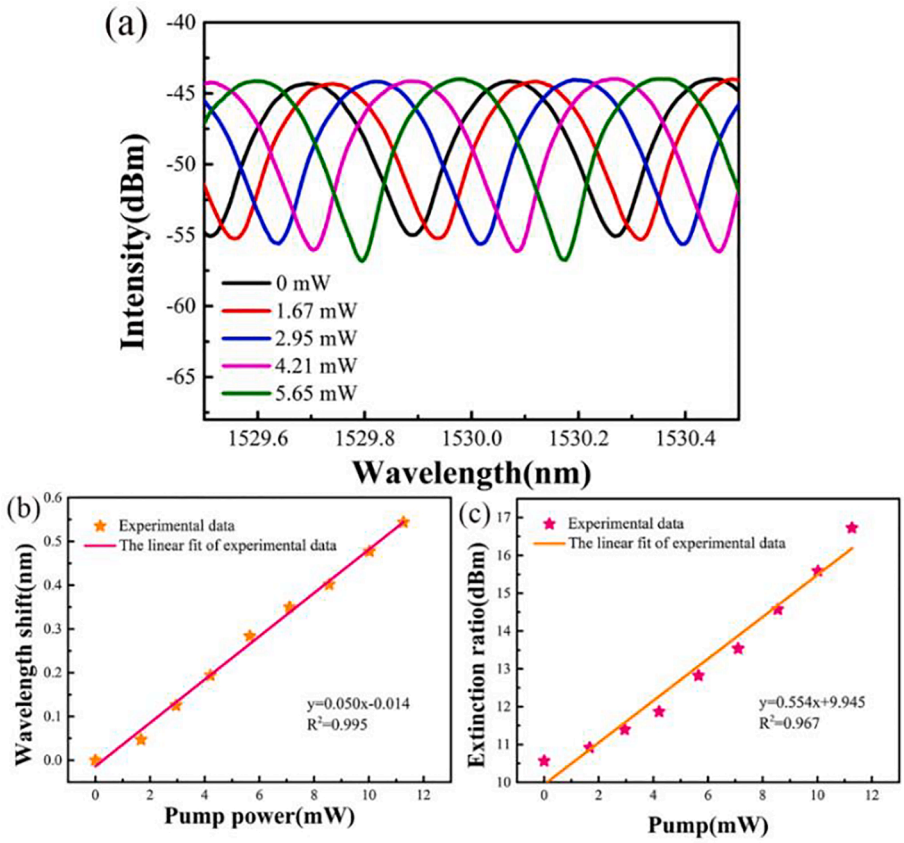

Fig 3. (a) Transmission spectra of the MXene-MCR with variations in the input pump power. (b) Resonance wavelength shift and (c) extinction ratio versus input pump power.

of MXene is changed by the external pump light power variation. On the other hand, as the pump light causes excitation, the MXene absorbs more light energy and electron-hole pairs are generated, which in turn produce photon generated carriers. At the same time, the photon generated carriers cause a variation in the real and imaginary parts of the refractive index and thus changes the complex refractive index of MXene [46]. The effective refractive index n_{eff} of the waveguide is also changed as the refractive index of MXene changes, which is reflected in the transmission properties, including changes in resonance wavelength and extinction ratio. The modulation sensitivity can be further improved by increasing the influence on n_{eff}, for example by reducing the fluidic channel thickness, optimizing the microfibre diameter and improving the quality of the MXene.

In order to further analyse the all-optical modulation properties of the MXene-MCR, the OSA was replaced by a standard photodetector and amplifier (Kemai, PDA, 10 GHz) whose output voltage was recorded using an oscilloscope (Tektronix MDO4054-6, 5 GHz/s), as shown in Fig. 5(a). The full pump probe system is illustrated in Fig. 5(a). An optical chopper was inserted between the TL and the 90% port of the coupler by replacing a section of the fibre connect to the coupler with a free-space optics lens system to transmit the narrow-band chopper modulated pump light signal into the MXene-MCR. The pump light from the tunable laser was thus modulated with a discrete square wave-like time signal with a frequency in the range 50 Hz–400 Hz at intervals of 50 Hz as provided the photo-chopper. The output light signal was converted to an electrical signal by the photodetector and amplifier and its output was recorded on the digital storage oscilloscope. A fibre Bragg grating (FBG) was added between the MCR and photodetector to filter out the pump light, and the transmission spectrum of the FBG is shown in Fig. 5(b). The loss peak spectral position of the FBG is located at the wavelength 1547.78 nm, and the center wavelength of the tunable laser was adjusted to the same position. Fig. 5(c) shows the temporal light modulation characteristic with a frequency of 150 Hz at room temperature. The extinction ratio of the modulated signal, the output light of MXene-MCR after filtering, diminishes compared to the pump light, which indicates that the MXene-MCR behaves as an all-optical modulator. The frequency of the signal light and pump light are almost identical. The rise and fall times, defined as the time taken to transition between the 10% low level and the 90% high level, were measured as 0.179 ms and 0.145 ms respectively, for a pulse input power 14.87 mW of the pump and chopped at a frequency of 150 Hz.

A comparison of the important parameters (including phase shift sensitivity, rise time and fall time) for recent all-optical modulators based on various microfibre structures and 2D materials is presented in Table 1. It can be seen that the phase shift sensitivity is better than other microfibre devices formed using different materials, which is primarily attributable to the longer light-matter interaction length of the MCR. In addition, the response time is faster than those reported for microfibre modulators, which mainly benefits from the small microfibre diameter and hollow rod thickness. Specifically, the small microfibre diameter and hollow rod thickness assist thermal conversion and dissipation.

Fig. 6 shows the relationship between the temporal pulse characteristics, pump power and the chopped frequency. For the output waveforms, the pump power influences the intensity and the frequency affects the periodically repeating waveforms, which manifests as pulse width. Fig. 6(a) shows the experimental results for a chopped frequency of 400 Hz at various pump light powers, which indicate that the intensity rises as the pump power increases, as shown in Fig. 6(b). Fig. 6(c) shows the experimental results for a pump power of 5.65 mW at various photo-chopper frequencies. Fig. 6(d) shows that the pulse width reduces as the chopped frequency increases, and continues to decrease, eventually approaching a minimum saturated value. Therefore, it can be seen

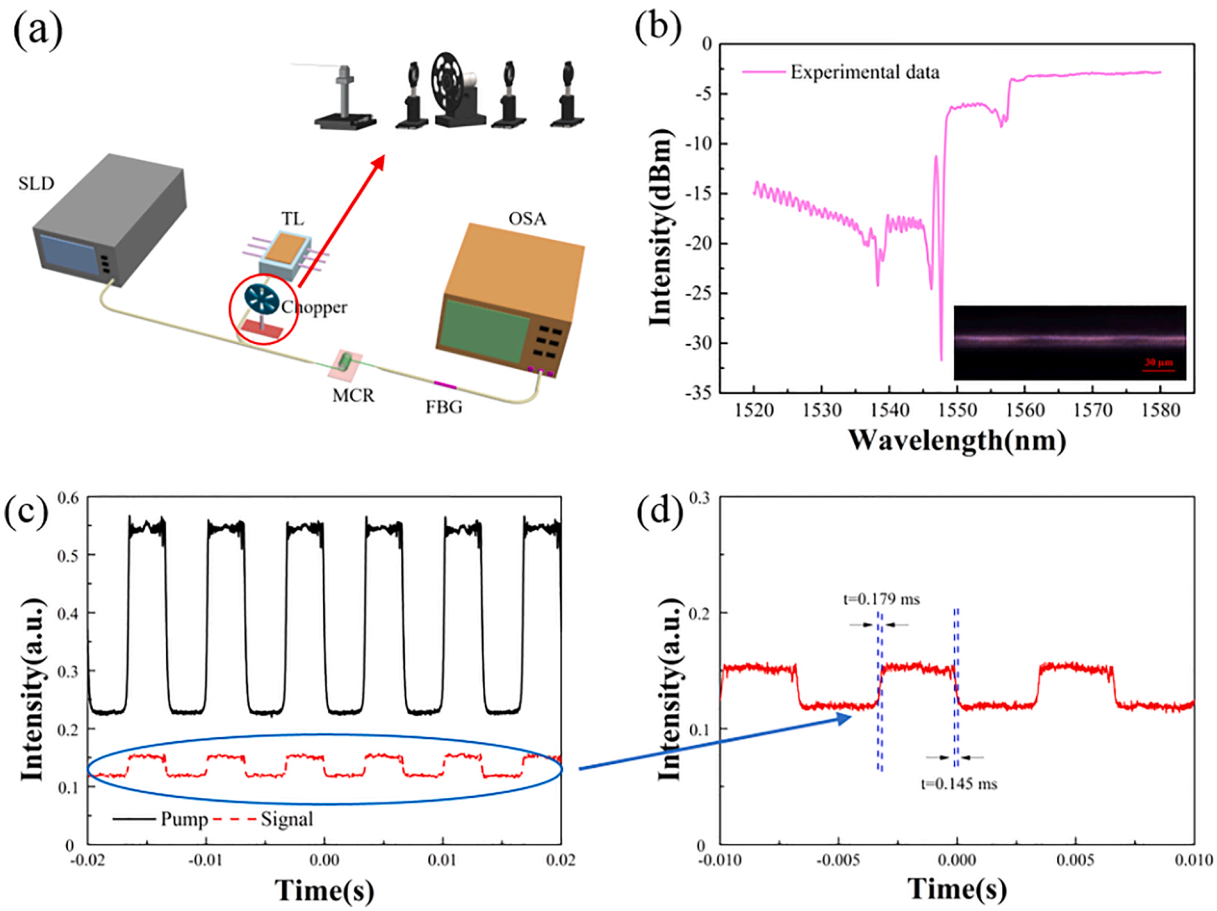

Fig 5. (a) Experimental setup for further characterization of all-optical modulation properties based on MXene-MCR. (b) Transmission spectrum of the FBG for filtering. The inset is the microscope image of the FBG. (c) Waveform comparison of the pump light and signal light (SLD light after modulated by chopper) at pump power levels of 14.87 mW and chopper frequency of 150 Hz. (d) Transient response time for the pulses for 14.87 mW pump power and 150 Hz chopper frequency.

Table 1
Comparison of all-optical modulator based on microfibre structure with existing technologies.

Microfibre structure	2D material	Sensitivity (π/mW)	Rise time (ms)	Fall time (ms)	Reference
Microfibre	graphene	0.192	9.1	3.2	[47]
Tapered fibre	WS_2	0.0174	7.3	3.5	[48]
MZI	fluorinated phosphorene	0.029	2.5	2.1	[49]
MI	MXene	0.043	4.5	3.9	[38]
MZI	MXene	0.061	4.10	3.55	[39]
MKR	MXene	0.196	0.306	0.301	[40]
MCR	MXene	0.262	0.179	0.145	This work

that both the intensity and width eventually stabilize with the increase of the corresponding input control parameters. In the case of the pulse width, the reason is that the rise and fall times limit the switching performance at the higher photo-chopper frequencies, and in the case of intensity, the reason is that the number of photon carriers generated from absorption of MXene depends on the amount of MXene resulting in an upper limit. The MXene based device has been demonstrated to be an excellent saturable absorption device. According to the principle of saturable absorption, the pump light changes the carrier distribution of electrons in the valence and conduction bands, further reducing the absorption of the pump power, and increasing the signal light intensity. Therefore, based on the dependence of the signal light intensity on the pump power, tunable optical filters, all-optical switches, all-optical modulators, and ultra-fast nonlinear processing can be developed based on the MXene-MCR, and it is possible to realize the adjustment of the optical switch ratio by controlling the pump power.

4. Conclusion

In conclusion, an all-optical modulation device based on MXene-MCR has been experimentally demonstrated. The MXene-MCR was fabricated by depositing the MXene on the fluidic channel of the MCR based on a photodeposition process and the modulation depth, resonance wavelength and extinction ratio of the output spectra were modulated by the tunable laser with a center wavelength of 1550 nm based on photo-thermal effect and absorption of MXene. The sensitivities of the resonance wavelength, phase shift and extinction ratio for pump power were recorded as 50 pm/mW, 0.262 π/mW and 0.554 dBm/mW respectively for the MXene-MCR. The all-optical modulation properties were further characterized by adding an optical chopper based on a free space lens coupling method as a control light source. The measured response time of the resulting light signal for rise and fall were 0.179 and 0.145 ms, respectively. The intensity and width of the light signal can also be modulated using only the control light, which shows that MXene has excellent nonlinear effects and therefore the MXene-MCR has the potential to be well suited for future use in ultra-fast optical nonlinear processing applications. The modulation properties may be further improved by adjusting the microfibre diameter and hollow rod thickness. The MXene-MCR has several advantages including excellent modulation properties, all-fibre construction, compact structure, easy fabrication, fast response, which make MXene-MCR potential

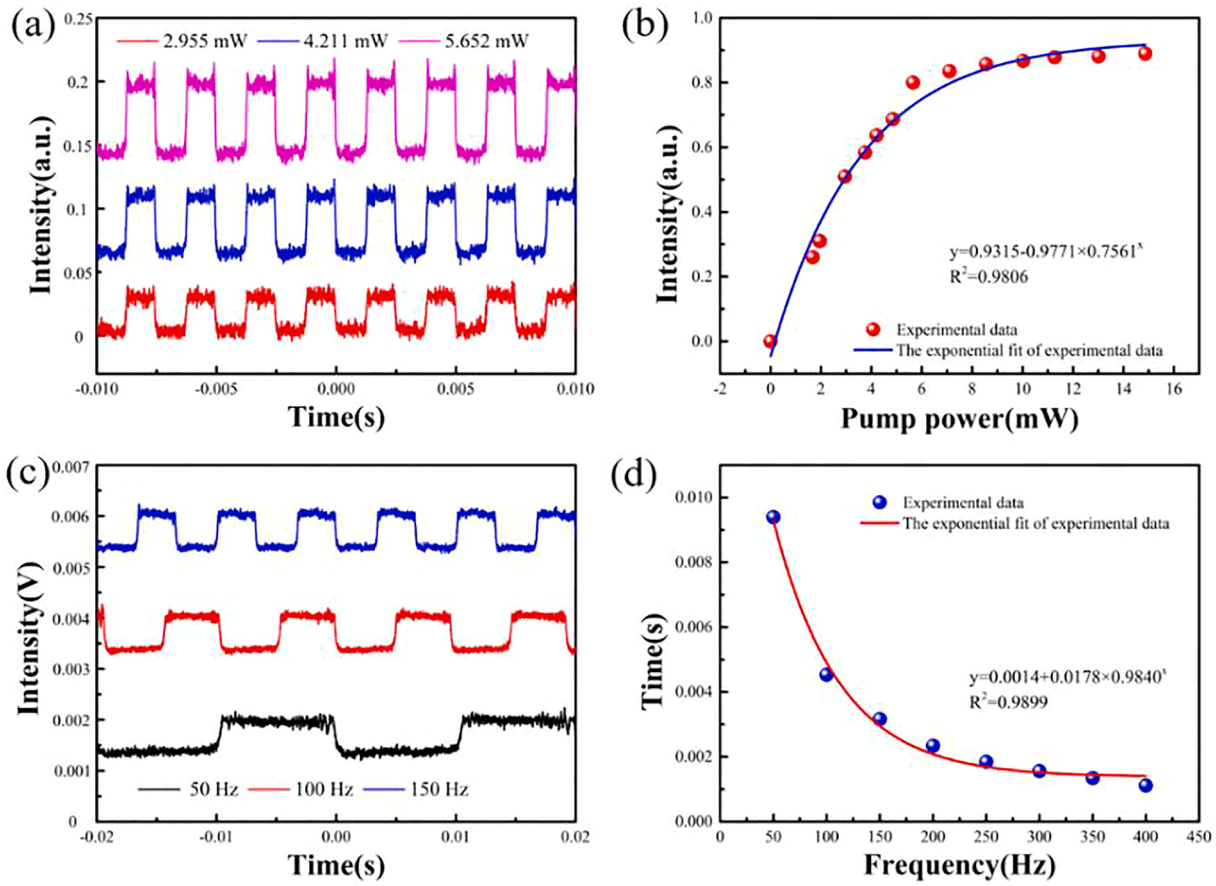

Fig 6. (a) Waveforms for various pump light power values. (b) Pulse intensity versus pump light power. (c) Waveforms for various photochopper frequencies. (d) Pulse width versus photochopper frequency.

in the application of tunable optical filters, optical switches and all-optical modulators.

Funding

Shenzhen Basic Research Program (JCYJ20190808140805488), Shenzhen Basic Research Project (JCYJ20190808173619062), National Key program of Natural Science Foundation of China (NSFC 61935006, 62090062), the 111 project (B13015) to the Harbin Engineering University, Heilongjiang Touyan Innovation Team Program. Professor Elfed Lewis is supported by Science Foundation Ireland under the Centres research program (SFI/12/RC/2302_P2) for the MaREI project.

Declaration of Competing Interest

The authors declare that they have no known competing financial interests or personal relationships that could have appeared to influence the work reported in this paper.

References

[1] N. Farrington, G. Porter, S. Radhakrishnan, H.H. Bazzaz, V. Subramanya, Y. Fainman, G. Papen, A. Vahdat, Helios: a hybrid electrical/optical switch architecture for modular data centers, SIGCOMM Comput. Commun. Rev. 40 (4) (2010) 339–350.

[2] S. Yao, S.J.B. Yoo, B. Mukherjee, S. Dixit, All-optical packet switching for metropolitan area networks: opportunities and challenges, IEEE Commun. Mag. 39 (3) (2001) 142–148.

[3] R. Rejeb, M. Leeson, R. Green, Fault and attack management in all-optical networks, IEEE Commun. Mag. 44 (11) (2006) 79–86.

[4] M.C. Soriano, P. Colet, C.R. Mirasso, Security Implications of Open- and Closed-Loop Receivers in All-Optical Chaos-Based Communications, IEEE Photonics Technol. Lett. 21 (7) (2009) 426–428.

[5] A. Detti, M. Listanti, Impact of segments aggregation on TCP Reno flows in optical burst switching networks, in: International Conference on Computer Communications, 2002, vol. 3, pp. 1803–1812.

[6] S. Armaghani, S. Khani, M. Danaie, Design of all-optical graphene switches based on a Mach-Zehnder interferometer employing optical Kerr effect, Superlattices Microstruct. 135 (2019), 106244.

[7] Y. Song, et al., Few-layer antimonene decorated microfiber: ultra-short pulse generation and all-optical thresholding with enhanced long term stability, 2D Mater. 4 (4) (2017), 045010.

[8] Q. Bao, et al., Atomic-Layer Graphene as a Saturable Absorber for Ultrafast Pulsed Lasers, Adv. Funct. Mater. 19 (19) (2009) 3077–3083.

[9] J. Zheng, et al., Few-Layer Phosphorene-Decorated Microfiber for All-Optical Thresholding and Optical Modulation, Adv. Opt. Mater. 5 (9) (2017) 1700026.

[10] M.J. Holmes, D.L. Williams, R.J. Manning, Highly nonlinear optical fiber for all optical processing applications, IEEE Photon. Technol. Lett. 7 (9) (1995) 1045–1047.

[11] Q. Xu, M. Lipson, All-optical logic based on silicon micro-ring resonators, Opt. Express 15 (3) (2007) 924–929.

[12] Y.-C. Chang, Y.-H. Lin, J.-H. Chen, G.-R. Lin, All-optical NRZ-to-PRZ format transformer with an injection-locked Fabry-Perot laser diode at unlasing condition, Opt. Express 12 (19) (2004) 4449–4456.

[13] K. Yamada, H. Fukuda, T. Tsuchizawa, T. Watanabe, T. Shoji, S. Itabashi, All-optical efficient wavelength conversion using silicon photonic wire waveguide, IEEE Photon. Technol. Lett. 18 (9) (2006) 1046–1048.

[14] G.-R. Lin, et al., Si-rich SiN x based Kerr switch enables optical data conversion up to 12 Gbit/s, Sci. Rep. 5 (1) (2015) 1–7.

[15] C.-L. Wu, et al., Enhancing optical nonlinearity in a nonstoichiometric SiN waveguide for cross-wavelength all-optical data processing, ACS Photon. 2 (8) (2015) 1141–1154.

[16] A. Pasquazi, et al., All-optical wavelength conversion in an integrated ring resonator, Opt. Express 18 (4) (2010) 3858–3863.

[17] C.-L. Wu, S.-P. Su, G.-R. Lin, All-optical modulation based on silicon quantum dot doped SiOx: Si-QD waveguide, Laser Photon. Rev. 8 (5) (2014) 766–776.

[18] S. Yu, et al., Graphene decorated microfiber for ultrafast optical modulation, Opt. Express 23 (8) (2015) 10764–10770.

[19] S. Yu, X. Wu, K. Chen, B. Chen, X. Guo, D. Dai, L. Tong, W. Liu, Y. Ron Shen, All-optical graphene modulator based on optical Kerr phase shift, Optica 3 (5) (2016) 541, https://doi.org/10.1364/OPTICA.3.000541.

[20] M. Sagues, A. Loayssa, Orthogonally polarized optical single sideband modulation for microwave photonics processing using stimulated Brillouin scattering, Opt. Express 18 (22) (2010) 22906–22914.
[21] D. Zhang, M.N. Slipchenko, D.E. Leaird, A.M. Weiner, J.-X. Cheng, Spectrally modulated stimulated Raman scattering imaging with an angle-to-wavelength pulse shaper, Opt. Express 21 (11) (2013) 13864–13874.
[22] Y. Wang, Q.-L. Wang, S. Zhou, J.-F. Wu, Y.-H. Wu, Analysis of thermo-optic effect-based refractive index dynamic modulation in microspherical resonator, Appl. Opt. 54 (28) (2015) 8363–8368.
[23] Ö. Boyraz, P. Koonath, V. Raghunathan, B. Jalali, All optical switching and continuum generation in silicon waveguides, Opt. Express 12 (17) (2004) 4094–4102.
[24] C.-L. Wu, S.-P. Su, G.-R. Lin, All-Optical Data Inverter Based on Free-Carrier Absorption Induced Cross-Gain Modulation in Si Quantum Dot Doped SiO2 Waveguide, IEEE J. Sel. Top. Quantum Electron. 20 (4) (2013) 323–331.
[25] R.D. Kekatpure, M.L. Brongersma, Quantification of free-carrier absorption in silicon nanocrystals with an optical microcavity, Nano Lett. 8 (11) (2008) 3787–3793.
[26] Y.-W. Hsueh, C.-H. Cheng, C.-S. Fu, H.-Y. Wang, B.-J. Huang, G. Lin, 4-QAM OFDM Data Switching via Free Carrier Absorption in Si-Rich SiC Waveguide, IEEE J. Sel. Top. Quantum Electron. 27 (3) (2021) 1–11.
[27] J. Lou, Y. Wang, L. Tong, Microfiber Optical Sensors: A Review, Sensors 14 (4) (2014) 5823–5844.
[28] G. Brambilla, F. Xu, P. Horak, Y. Jung, F. Koizumi, N.P. Sessions, E. Koukharenko, X. Feng, G.S. Murugan, J.S. Wilkinson, D.J. Richardson, Optical fiber nanowires and microwires: fabrication and applications, Adv. Opt. Photonics 1 (1) (2009) 107, https://doi.org/10.1364/AOP.1.000107.
[29] Y. Yin, et al., Investigation of temperature dependence of microfiber coil resonators, J. Lightwave Technol. 36 (20) (2018) 4887–4893.
[30] S. Li, Y.u. Yin, E. Lewis, G. Garrell, P. Wang, A twelve-wavelength Thulium-doped fibre laser based on a microfibre coil resonator incorporating black phosphorus, Opt. Commun. 437 (2019) 342–345.
[31] R. Ismaeel, T. Lee, F. Alsaab, Y. Jung, G. Brambilla, A multi-port optical microfiber coil resonator, in: Conference on Lasers and Electro Optics, 2012, pp. 1–2.
[32] Y. Yin, S. Li, P. Wang, All-Optical Tuning of Au Nanocluster Functionalized Microfibre Coil Resonator, in: Journal of Physics: Conference Series, 2021, vol. 1892, no. 1: IOP Publishing, p. 012026.
[33] C. Ma, et al., Theoretical and experimental study of structural slow light in a microfiber coil resonator, Appl. Opt. 54 (18) (2015) 5619–5623.
[34] J.-H. Chen, B.-C. Zheng, G.-H. Shao, S.-J. Ge, F. Xu, and Y.-Q. Lu, An all-optical modulator based on a stereo graphene–microfiber structure, Light: Sci. Appl. 4(12) (2015) e360–e360.
[35] L. Wu, et al., Few-layer tin Sulfide: a promising black-phosphorus-analogue 2D material with exceptionally large nonlinear optical response, high stability, and applications in all-optical switching and wavelength conversion, Adv. Opt. Mater. 6 (2) (2018) 1700985.
[36] H. Ahmad, H.S. Lim, M.Z. Matjafri, Y.Q. Ge, H. Zhang, Z.C. Tiu, All-fiber optical polarization modulation system using MoS2 as modulator, Infrared Phys. Technol. 102 (2019), 103002.
[37] G. Chen, et al., Highly sensitive all-optical control of light in WS2 coated microfiber knot resonator, Opt. Express 26 (21) (2018) 27650–27658.
[38] C. Wang, et al., MXene Ti3C2Tx: A Promising Photothermal Conversion Material and Application in All-Optical Modulation and All-Optical Information Loading, Adv. Opt. Mater. 7 (12) (2019) 1900060.
[39] Q. Wu, et al., MZI-Based All-Optical Modulator Using MXene Ti3C2Tx (T = F, O, or OH) Deposited Microfiber, Adv. Mater. Technol. 4 (4) (2019) 1800532.
[40] Q. Wu, et al., All-Optical Control of Microfiber Knot Resonator Based on 2D Ti2CTx MXene, Adv. Opt. Mater. (2020) 1900977.
[41] H. Xin, B. Li, Targeted delivery and controllable release of nanoparticles using a defect-decorated optical nanofiber, Opt. Express 19 (14) (2011) 13285–13290.
[42] M. Sumetsky, Optical fiber microcoil resonators, Opt. Express 12 (10) (2004) 2303–2316.
[43] L. Tong, J. Lou, E. Mazur, Single-mode guiding properties of subwavelength-diameter silica and silicon wire waveguides, Opt. Express 12 (6) (2004) 1025–1035.
[44] J.J. Bae, et al., Sensitive photo-thermal response of graphene oxide for mid-infrared detection, Nanoscale 7 (38) (2015) 15695–15700.
[45] S.-S. Yun, J.-H. Lee, A micromachined in-plane tunable optical filter using the thermo-optic effect of crystalline silicon, J. Micromech. Microeng. 13 (5) (2003) 721–725.
[46] Y. Xiao, et al., Theoretical investigation of optical modulators based on graphene-coated side- polished fiber, Opt. Express 26 (11) (2018) 13759–13772.
[47] X. Gan, C. Zhao, Y. Wang, D. Mao, L. Fang, L. Han, J. Zhao, Graphene-assisted all-fiber phase shifter and switching, Optica 2 (5) (2015) 468, https://doi.org/10.1364/OPTICA.2.000468.
[48] K. Wu, C. Guo, H. Wang, X. Zhang, J. Wang, J. Chen, All-optical phase shifter and switch near 1550nm using tungsten disulfide (WS2) deposited tapered fiber, Opt. Express 25 (15) (2017) 17639–17649.
[49] Y. Wang, et al., All-Optical Phosphorene Phase Modulator with Enhanced Stability Under Ambient Conditions, Laser Photon. Rev. 12 (6) (2018) 1800016.